

We are IntechOpen, the world's leading publisher of Open Access books Built by scientists, for scientists

6,900

Open access books available

186,000

International authors and editors

200M

Downloads

Our authors are among the

154

Countries delivered to

TOP 1%

most cited scientists

12.2%

Contributors from top 500 universities



WEB OF SCIENCE™

Selection of our books indexed in the Book Citation Index
in Web of Science™ Core Collection (BKCI)

Interested in publishing with us?
Contact book.department@intechopen.com

Numbers displayed above are based on latest data collected.
For more information visit www.intechopen.com



Solar Energy in Industrial Processes

Guillermo Martínez-Rodríguez and Amanda L. Fuentes-Silva

Abstract

A design methodology to integrate solar heat into industrial process is showed in this chapter, attending restrictions like availability for area of installation, economic, environmental, and operating conditions. The evaluation of each of the restrictions allows responding to real situations that arise in the industrial sector and thereby determining the scenario that best suits the industry. To achieve this objective, the evaluation of two real scenarios was carried out; in the first one there are no installation area limitations, while in the second, only the 50% of required installation area is available. The results obtained when evaluating the scenarios exhibit a direct relationship between the available space, the capital of the investment and the CO₂ emissions, but this is not reflected in the same proportion in the operation of the process. In scenario one, the payback of the integrated system is 5.99 years with zero emissions to the atmosphere. For scenario two, the reduction of CO₂ emissions is 80.62% with a recovery time of the investment of the integrated system of 2.61 years. In this context, Chemical Vapour Deposition is proposing as a innovative technology to improve the solar devices efficiency.

Keywords: solar collector network, spatial restriction, payback time, thermal solar heat integration, real scenarios to integrate solar heat

1. Introduction

Industrial sector demands large amounts of energy, two thirds of it is in the form of heat [1]. Of the heat demand in industry, almost half, 48%, is required for high temperature heat (more than 400 °C) mainly in the intensive industries of iron and steel and other minerals, which reach temperatures of up to 1450 °C; chemical and petrochemical, 900 °C; among others, 22% is used for medium-temperature heat (150 to 400 °C) and the remaining 30% is used for low-temperature heat (less than 150 °C) [2]. Currently, only 9% of the heat demand of industrial processes is supplied from renewable energy sources, 79% of solar thermal installations use flat plate solar collectors and evacuated tubes, 11% correspond to the use of parabolic-cylinder collectors, and the remaining percentage of other technologies [3]. Chemical Vapour Deposition, CVD, plays an important role in the development and improvement of solar technology. CVD technologies have been innovating for at least 50 years to increase the efficiency of solar energy collection, both from solar cells and, more recently, from evacuated tubes [4].

When a protocol to solar heat for process industrial integration (SHIP integration) is being designed, there are some parameters that determine the solar heat integration potential: a) inherent to the process: energy demand [5], hourly heat

demand profile, seasonal heat demand profile [6], temperature intervals, continuous, semicontinuous or batch processes, different kinds of solar heat (steam, drying, hot water) [7]; b) regarding to the facilities: location [5], surface area availability; c) depending on the expected objectives: solar fraction, outlet temperatures, payback time, lower emissions of greenhouse gases (GHG), saving costs [8]. However, the picture is not complete if the limitations or restrictions that represent serious challenges to overcome to achieve efficient use of solar energy are not given equal importance: a) inherent to the process: higher process heat demand than solar heat produced; b) regarding to the facilities: limited flexibility of the systems, use of outdated or non-optimal technology for process conditions, higher costs of solar heating systems than fossil fuel conventional systems [6]. And all these considerations must in turn take into account energy policy and the associated investment, which can also limit or restrict the optimal use of solar energy: lack of economic support to research and innovation to tuning and updating of technology, lack of standard procedures for the implementation and evaluation of technological systems, difficulty promoting attractive investment and business models for the deployment and integration of renewable energies, and few market incentives [9], prohibitions to produce and distribute renewable heat [10], among other.

With the technologies that currently exist for the use of solar energy for heat production, the processes that demand low-temperature heat are the most convenient for integrating solar heat [11], besides, when solar storage is introduced, solar fraction increases markedly compared to a process without storage [5].

The evaluation of some of the restrictions or limitations such as: available installation space for the collector network, availability of capital or the low prices of the fossil fuels used and the supply time of the collector network, allows to evaluate the real impact of each scenario when compared with the one where there are no restrictions for the installation of the solar thermal device and thus seek the profitability of the device in whatever the scenario. Next, the proposed methodology for the integration of solar thermal energy with some real restrictions is described.

The objective of this chapter is to make a general approach that includes some real scenarios that arise when solar thermal energy is integrated into industrial processes, whether they operate continuously or in batches.

2. Methodology for the integration of solar thermal energy

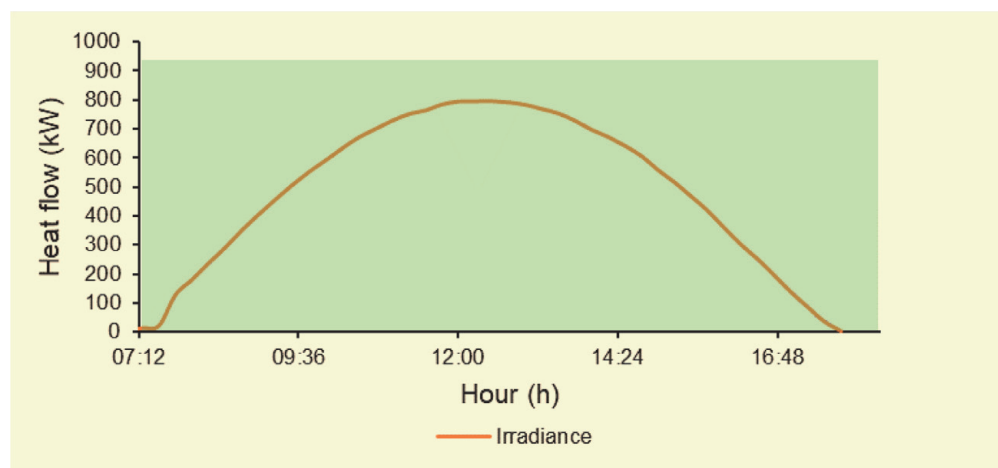
The integration of solar thermal energy must be economically attractive to compete with fossil fuels and it must be flexible in such a way that it can be applied to various real scenarios where there are spatial, economic, operational, and environmental limitations, limiting the amount of solar energy that can be supplied and with it the solar fraction. The irradiance levels of the site constitute a variable that can limit the maximum output temperatures that a network of solar collectors can reach in a period to guarantee the temperature level and the supply of the total or partial thermal load. Any of the previously stated limitations can define the integration of solar thermal energy.

Whatever the application, the integration of solar thermal energy must be cost-effective and environmentally friendly by reducing the generation of greenhouse gases. Although any reduction in the generation of greenhouse gases is an important point for any industrial sector, the design objective should always be the total elimination of the use of fossil fuels. However, the limitations to achieve a solar fraction of unity are real and it is important to evaluate how they can define the installation of the solar thermal device. Each of the restrictions raised is a challenge that must be addressed and resolved to respond to the real needs that arise in the

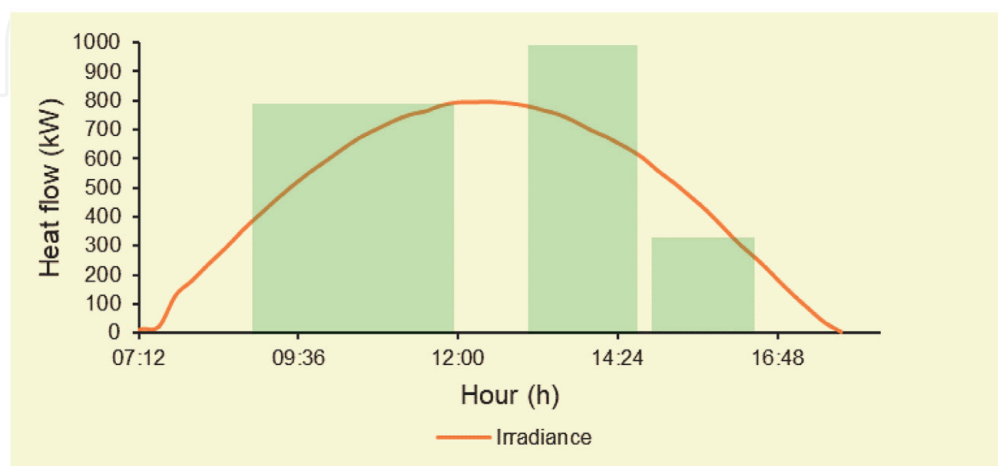
industrial sector when the transition towards the use of renewable energies is sought to replace fossil fuels.

The methodology developed is general and can be used or coupled to medium temperature solar collectors or mixed systems (low and medium temperature solar collector technologies) for a specific application. The range of applications can be expanded by defining some other objectives of industrial interest.

The approach contemplates the integration of solar thermal energy into a real case, using low-temperature solar collectors, specifically, flat plate solar collectors, for the selection, design, and operation of the collector network. On the other hand, the design of the collector network is based on the most critical conditions of the year, which correspond to the winter period and guarantee the supply of the thermal load throughout the year. It is important to mention that the rest of the year there will be surplus energy that can be used in other applications. In the selected case study, two scenarios will be evaluated. In the first scenario, the total supply of the thermal load is considered at the temperature level required by the process, with a solar fraction of one and zero greenhouse gas emissions to the environment. In this scenario there are no space limitations for the installation of the solar collector network. In the second scenario, it is proposed that only 50% of the area required for the total supply of the thermal load is available, reducing the fraction as the generation of greenhouse gases. In this last scenario, it is analysed how the restrictions impact and what implications it has with the rest of the variables such as:



a)



b)

Figure 1. Main stages that require thermal energy in an industrial process (green colour): Continuous process (a), batch process (b).

reduction in emissions, time in the recovery of investment (payback time) and time of direct supply of the collector network.

To carry out the integration of solar thermal energy, it is important to quantify the available solar resource to determine the maximum outlet temperature of the solar collector network, determining the supply time at target temperature and the size of the network. For a batch process, it would be sought that the direct supply time from the network is equal to the time required by the process, otherwise it is necessary to match the availability of the solar resource with the energy requirement of the process at the temperature required by it.

In **Figure 1**, reference is made to the energy requirements of an industrial process and to solar availability, to match these requirements and to be able to integrate solar thermal energy. For the solar energy supply or production curve, it is considered that there is an available area of 1000 m^2 . Section a) represents a continuous process and the energy demand of the process is above the amount that is captured with the available surface (1000 m^2), to supply the thermal load, the capture area would be increased. In part b) a batch process is shown where it is observed that the energy requirement can be provided entirely by solar energy.

In this approach it is possible to supply the thermal energy of the process through solar thermal energy using a thermal storage system to match the demand and energy production. The temperature level required for each process operation is not considered in the diagram.

Figure 2 displays the temperature level required by the process and the temperature provided by the solar collector network. It is observed that during a period of 5 h 45 min (9:45 h - 15:30 h) the target temperature of the process is reached. In the time that the requirement does not coincide with the solar availability, the thermal load would be supplied with the use of storage.

In parallel, the Pinch Analysis methodology can be used, and the energy requirement of the process can be reduced by favouring the process-process heat exchange. These objectives were raised and solved in the work published by Fuentes-Silva et al. [8]. On the other hand, ΔT_{min} is a function of auxiliary services, when increasing the heat recovery area, it is reduced, however, the area of the collector network increases, so it is interesting to evaluate the costs associated with this relationship.

Figure 3 presents the logic of the proposed methodology for the integration of solar thermal energy into industrial processes, it is represented by a block diagram. The proposed methodology is carried out in some stages simultaneously and feedback is provided until the best conditions for the final design are reached.

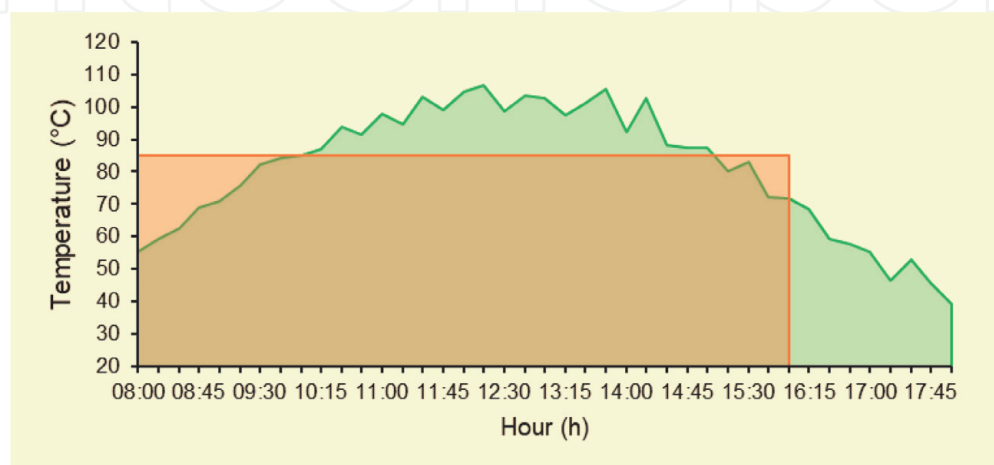


Figure 2.
Temperature level required by the process (85 °C) and that supplied by the solar collector network (variable).

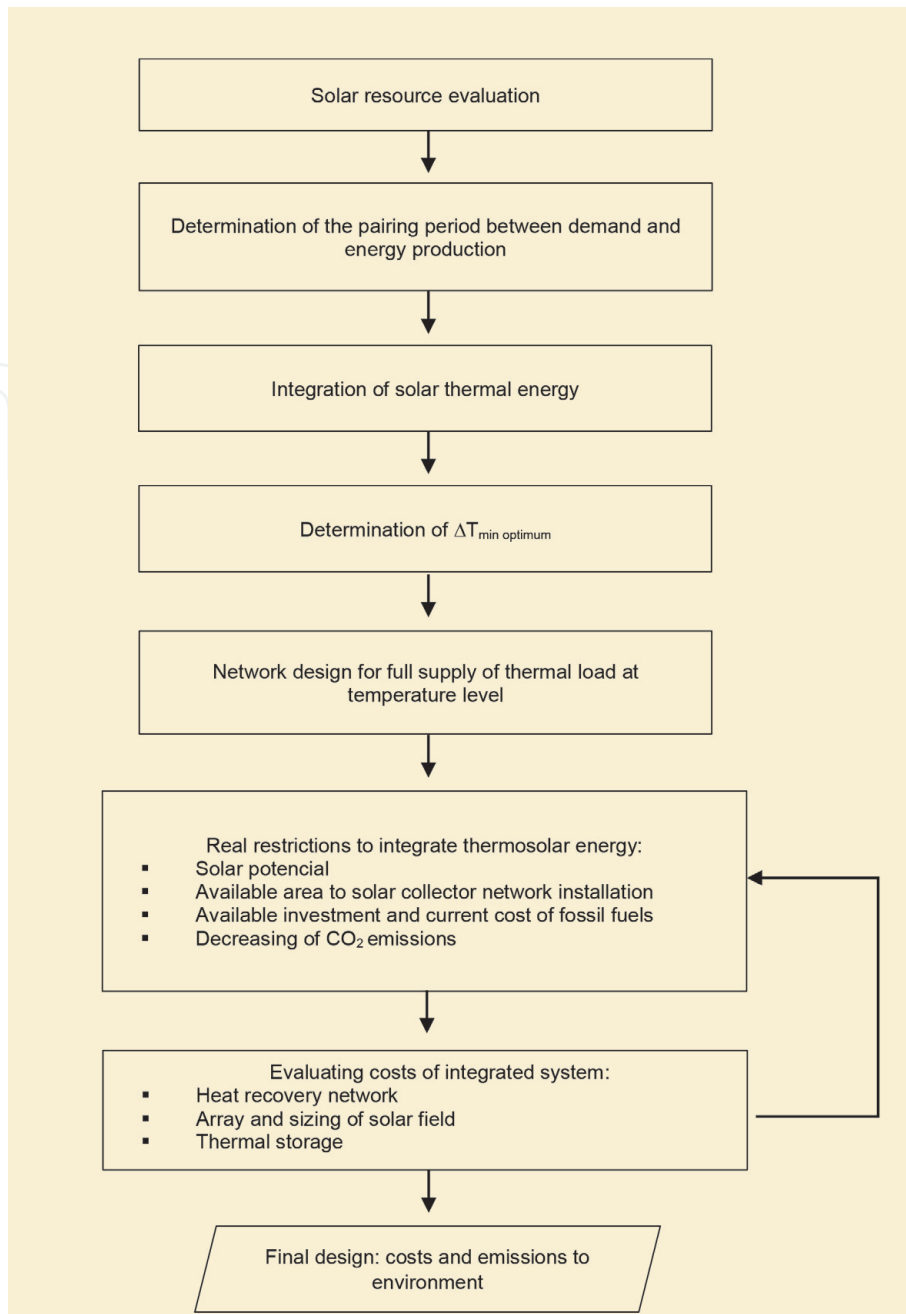


Figure 3.
 Design algorithm to integrate solar thermal energy.

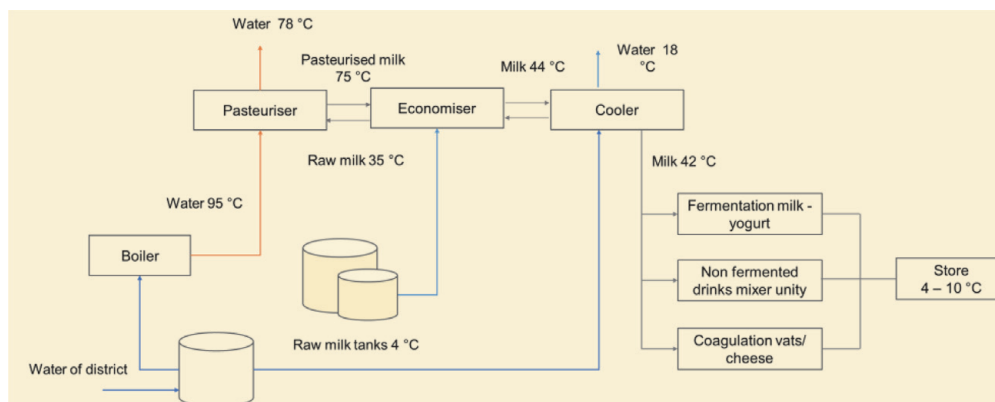


Figure 4.
 Flow diagram of dairy process.

2.1 Case study

The case study is a dairy process described in the literature [12]. It operates on batch and the required heat utility is from 8:00 h to 13:00 h (five hours), enough to carry out pasteurisation of milk at 85 °C. Hot water is needful to curd the milk from 8:30 h to 13:00 h (4.5 hours) at 40 °C; more hot water is required at 62 °C to clean the equipment during a period of 2 hours (16:00 h – 18:00 h). **Figure 4** represents the diverse production stages in a dairy plant at required temperatures.

In **Figure 5** the periods of demand for thermal energy of the main operations of the process are shown (squares) and the period of solar energy production is also displayed (parabolic line). **Figure 5** shows the pairing periods, and this allows to determine if the heat supply is direct from the solar collector network or if requires storage, it also helps to define the possible heat exchanges between the process streams to recover energy.

2.2 Energy integration of the process

Next, Pinch Analysis is used to carry out the integration of solar thermal energy and determine the optimal ΔT_{min} .

Dairy process stream data is shown in **Table 1** including inlet and outlet temperatures and heat capacity. From the data of the currents, the Composite Curves are constructed and determine the minimum hot and cold utilities, and thus the process-process heat exchanges. To deliver the thermal load required by the process, a boiler that produces hot water at 95 °C for 5 hours is used, providing a thermal load of 4,401.01 kWh. The heat transfer coefficients used are 0.8 kW/m² °C for water and slightly viscous substances and 0.3 kW/m² °C for viscous substances.

The Composite Curves provide a scheme of pure countercurrent heat transfer of the process streams for a chosen ΔT_{min} . They are used to determine the minimum heating and cooling requirements of the process and this allows the calculation of the minimum transfer area prior to the detailed design of the heat transfer network.

In **Figure 6** we have the Composite Curves for a ΔT_{min} of 10 °C where the minimum utilities are determined, which are 294.78 and 260.68 kW of heating and cooling, respectively. It is observed that the thermal load and the temperature level of the hot utility can be supplied by solar thermal energy.

Determination of the minimum area assumes that there is vertical heat exchange between the Composite Curves throughout the entire enthalpy range. In the graph of the Composite Curves, we can read the amount of heat that will be transferred

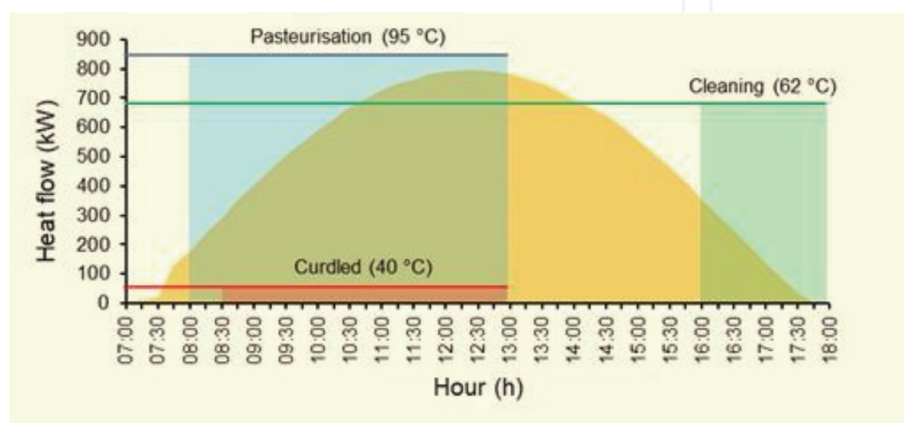


Figure 5.
Pairing between major process operations and available irradiance in a day.

Description	T _{inlet} (°C)	T _{outlet} (°C)	CP (kW/°C)
Mains water	12.20	38.00	2.64
Milk- rennets vats	34.00	35.00	3.89
Pasteurised milk- effluent	75.00	44.00	4.38
Water for boiler	95.00	78.00	10.63
Raw milk- input	4.00	35.00	4.38
Milk- input	35.00	75.00	4.38
Mains water- for cooler	12.20	18.00	6.35
Input milk	44.00	36.00	5.84
Water – of storage tank	73.30	40.00	1.94
Water – rennets vats	40.00	38.00	3.89
Water – of storage tank	62.40	25.00	9.30
Water – of storage tank, surplus	62.40	25.00	12.90
Main water -for boiler	12.20	95.00	10.63

Table 1.
 Stream data for dairy process

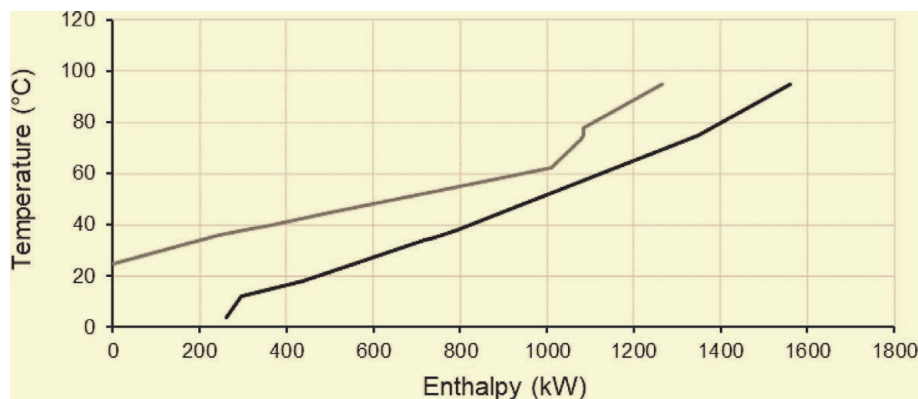


Figure 6.
 Composite curves for a ΔT_{min} of 10 °C.

between the streams, as well as the values of the outlet and inlet temperatures (at that interval) of the hot streams, like so the values of the outlet temperatures and entry of cold currents. So if the curves, both for hot and cold currents, correspond to only one of them, as happens between an exchange of process current - auxiliary service, we can estimate the necessary area of heat exchange given by Eq. (1) known as the Bath equation, which is based on the countercurrent heat exchange assumption implicit in the compound curves and this leads to the minimum area, only if the global heat transfer coefficients are equal for all exchanges [13].

$$A_{HRN} = \sum_k^{k \text{ intervals}} \frac{1}{\Delta T_{ML}} \left(\sum_i^{hot \ i} \frac{q_i}{h_i} + \sum_j^{cold \ j} \frac{q_j}{h_j} \right) \quad (1)$$

The estimate of the total A_{HRN} area is obtained by adding the area of each interval (m^2), q_i and q_j are the thermal exchange loads obtained from the enthalpies in the Composite Curves (kW). h_i and h_j are the individual transfer coefficients ($kW/m^2 \text{ } ^\circ C$). The subscripts k , i and j .

The calculated minimum area is used to determine the cost of the heat recovery network, C_{HRN} (USD), of the process based on Eq. (2).

$$C_{HRN} = N_e \left[26600 + 6500 \left(\frac{A_{HRN}}{N_e} \right)^{0.9} \right] \quad (2)$$

Where N_e is the number of equipment, A_{HRN} is the area of the heat recovery network (m^2) this value corresponds to the exchange area [14]. To determine the cost of auxiliary services, C_{AS} , Eq. (3), reported by [15].

$$C_{AS} = Q_h C_{ST} + Q_c C_{CO} \quad (3)$$

In Eq. (3) Q_h and Q_c are the minimum requirements for heating and cooling the process (kW), while C_{ST} and C_{CO} are the costs associated with steam and cooling water, respectively (USD/kW year). In this study, the cost of heating services is proposed to be 150 USD/kW year and cooling services 35 USD/kW year.

The total cost of the annualised heat recovery network, $C_{TA HRN}$ (USD/year), is obtained by adding the estimated cost of capital (C_{HRN}) and the annualised service costs (C_{AS}), given by Eq. (4)

$$C_{TA HRN} = f_A C_{HRN} + f_A C_{AS} \quad (4)$$

The annualisation factor f_A is calculated considering an annual interest of 5% for a period of 25 years. In this study, this value is considered as the number of years of useful life of a piece of equipment or a network of equipment. To find the optimal ΔT_{min} it is required to evaluate the total cost associated with each chosen ΔT_{min} . **Table 2** shows the results to determine the optimal ΔT_{min} in an interval from 1 to 30 °C, for each ΔT_{min} the minimum energy requirements, the heat exchange area and the annualised costs of: heat recovery (C_{HRNA}), auxiliary services (C_{ASA}) and the total cost of the heat recovery network ($C_{TA HRN}$).

In **Figure 7** the total cost of the heat recovery network is shown, it can be seen the optimal ΔT_{min} is located at 13 °C and the minimum energy requirements are: 339.81 kW and 305.71 kW, corresponding to the minimum services heating and cooling, respectively.

The design of the solar collector network will be carried out considering the optimal ΔT_{min} and its corresponding minimum hot utility (thermal load).

2.3 Solar resource available

The irradiance data and other environmental variables (ambient temperature and wind speed) were taken from a meteorological station of the Solar Energy Laboratory of the University of Guanajuato, Guanajuato city, Mexico. The geographical location of the meteorological station is latitude of 21°01'0" N, longitude 101°15'24" W, at an average sea level elevation of +2 000 meters, central time zone, UTC – 6 and in summer UTC – 5. **Figure 8** shows the radiation data throughout the year under clear sky.

2.4 Design of the solar collector network

The integration of solar energy in an industrial process presents a challenge for existing process integration techniques, due to the non-continuous nature of supply, available irradiance levels associated with direct supply time from the solar collector network to the process. The efficiency of solar technologies must be

ΔT_{min} (°C)	Q_h (kW)	Q_c (kW)	N_e	A_{HRN} (m ²)	C_{HRN} (USD)	C_{HRNA} (USD/y)	C_{ASA} (USD/y)	$C_{TA HRN}$ (USD/y)
1	159.69	125.65	17	531.63	3,199,987.73	227,046.99	28,351.41	255,398.40
2	174.70	140.66	17	428.05	2,721,302.35	193,083.09	31,128.26	224,211.35
3	189.71	155.67	17	369.75	2,446,943.96	173,616.69	33,905.11	207,521.80
4	204.72	170.68	17	329.89	2,256,861.40	160,129.86	36,681.96	196,811.82
5	219.73	185.63	17	301.89	2,121,959.05	150,558.21	39,456.78	190,014.99
6	234.74	200.64	17	278.22	2,006,954.08	142,398.32	42,233.63	184,631.95
7	249.75	215.65	17	258.87	1,912,212.04	135,676.14	45,010.48	180,686.62
8	264.76	230.66	17	242.64	1,832,205.01	129,999.45	47,787.33	177,786.78
9	279.77	245.67	17	228.77	1,763,388.35	125,116.74	50,564.18	175,680.92
10	294.78	260.68	17	216.70	1,703,160.69	120,843.44	53,341.03	174,184.47
11	309.79	275.69	17	206.12	1,650,130.10	117,080.79	56,117.88	173,198.67
12	324.80	290.70	17	196.77	1,603,030.89	113,738.98	58,894.73	172,633.71
13	339.81	305.71	17	188.45	1,560,908.19	110,750.27	61,671.58	172,421.85
14	354.82	320.72	17	180.99	1,522,985.26	108,059.55	64,448.43	172,507.98
15	369.83	335.73	17	174.26	1,488,643.65	105,622.92	67,225.28	172,848.20
16	384.84	350.74	17	168.16	1,457,391.84	103,405.53	70,002.13	173,407.66
17	399.85	365.75	17	162.60	1,428,847.98	101,380.28	72,778.98	174,159.26
18	414.86	380.76	17	157.53	1,402,675.38	99,523.27	75,555.83	175,079.10
19	429.87	395.77	17	152.88	1,378,625.23	97,816.85	78,332.68	176,149.53
20	444.88	410.78	17	148.61	1,356,470.80	96,244.94	81,109.53	177,354.47
21	459.89	425.79	17	144.67	1,336,008.06	94,793.05	83,886.38	178,679.43
22	474.90	440.79	17	141.04	1,317,077.19	93,449.86	86,662.92	180,112.78
23	489.91	455.81	17	137.69	1,299,526.66	92,204.61	89,440.08	181,644.69
24	504.92	470.82	17	134.58	1,283,244.98	91,049.38	92,216.93	183,266.31
25	521.52	487.41	18	130.09	1,293,338.46	91,765.54	95,286.82	187,052.36
26	539.17	505.12	18	125.69	1,270,040.65	90,112.50	98,554.10	188,666.60
27	556.82	322.05	19	121.57	1,281,326.20	90,913.24	94,794.15	185,707.39
28	576.80	542.75	18	117.34	1,225,502.94	86,952.45	105,516.39	192,468.84
29	596.01	561.96	18	113.47	1,204,793.70	85,483.07	109,069.50	194,552.57
30	613.66	579.61	18	110.03	1,186,270.01	84,168.77	112,334.75	196,503.52

Table 2.
Results of pinch analysis to determine optimal ΔT_{min} .

determined since it is influenced by the environmental conditions of the place, this must be evaluated to guarantee the supply of the hot utility. This methodology combines this information to lead to the design of the solar thermal installation to reach the target temperature required by the process and satisfy the thermal requirements of the process with the lowest cost and taking care of the restrictions that the process presents. This must be attractive to compete with fossil fuels.

The design of the solar collector network is based on the methodology proposed by Martínez-Rodríguez et al., [16] to supply the thermal load at the required process temperature level. The design variables of the low temperature solar collector

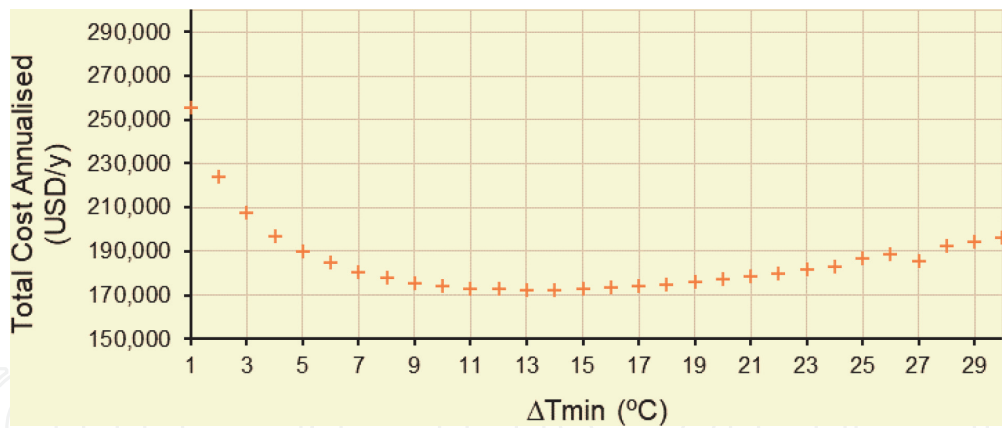


Figure 7.
Annualised total cost from heat recovery network against ΔT_{min} .

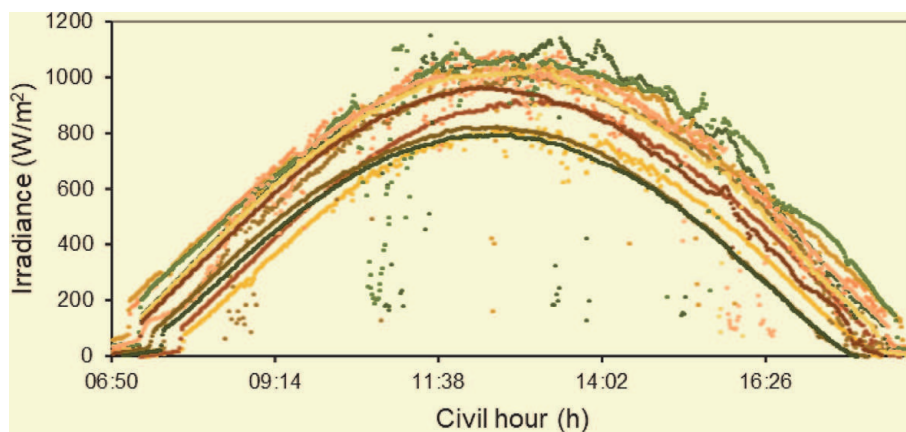


Figure 8.
Irradiance throughout a year for clear sky days.

network are the operating conditions of the process (temperature and required thermal load), the environmental parameters (irradiance and ambient temperature), geometric dimensions and characteristics of the flat-plate solar materials, the properties of the working fluid, and the network operating conditions (flow and feed temperature).

The minimum number of collectors connected in series can be calculated considering that the minimum difference between the outlet temperature of the fluid from the collector, T_o ($^{\circ}\text{C}$), and the temperature of the fluid at the entrance to the collector, T_i ($^{\circ}\text{C}$), is equal to or greater than 1°C . Generalising this difference for any collector or series have Eq. (5)

$$\Delta T = T_o^n - T_o^{n-1} \quad (5)$$

Where n refers to outlet temperature of the n -th element and $n-1$ refers to the outlet temperature of one minus to the n -th element ($^{\circ}\text{C}$) (**Figure 9**).

The number of branches or lines in parallel is calculated by Eq. (6)

$$N_p = \frac{Q_i}{Q} \quad (6)$$

Q_i is the thermal load provided by a series of n collectors connected in series (kW) and Q is the total thermal load (kW) required by the process, whether to cover partially or totally.

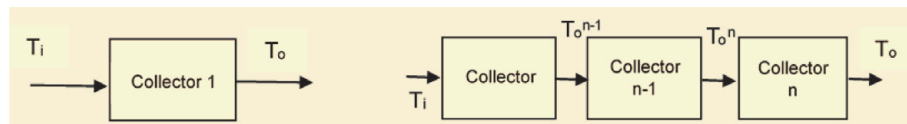


Figure 9.
 Series of n collectors.

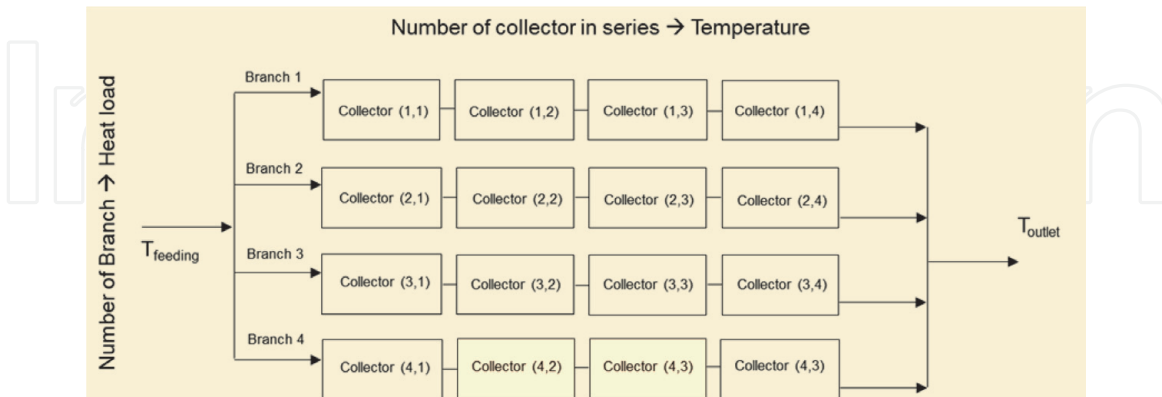


Figure 10.
 Structure of a solar collector network with 16 units.

Several solar collectors, N_c , make up the structure of the solar collector network as show Eq. (7)

$$N_c = N_p N_s \quad (7)$$

N_s is the number of series collectors and N_p is the number of parallel branches.

In **Figure 10** the arrangement of a network of 16 collectors in a 4 x 4 arrangement (parallel series) is displayed. Generalising the arrangement for any collector network it can be denoted as $m \times n$, where the lines in parallel to be placed (m) and the number of collectors connected in series (n) are shown. In this way, it is possible to meet the temperature level and the thermal load required for the process, of these, the first is achieved by connecting n collectors in series and the second is achieved through the determination of branches given by Eq. (6).

The absorber surface of the solar collector network is calculated from Eq. (8)

$$A_{SCN} = LWN_c \quad (8)$$

Where A_{SCN} is the area of the solar collector network (m^2), N_c is the number of collectors, L is the length (m), and W is the width of the solar collector (m).

Then we proceed to determine the cost of the collector network, C_{SCN} (USD), using Eq. (9) reported in [17]:

$$C_{SCN} = N_c \left[\gamma_0 + \frac{A_t N_t}{\pi} \left(\gamma_1 d + \gamma_2 + \frac{\gamma_3}{d} \right) + WL\gamma_4 + \gamma_{10} \frac{\dot{m}L\mu}{\pi\rho d^4} \right] + \gamma_5 \left(\frac{\dot{m}H_b}{eff} \right) \quad (9)$$

Where N_c is the number of collectors, A_t is the lateral area of the tube, N_t is the number of tubes, d is the internal diameter of a tube, W and L are the width and length of a solar collector, H_b and eff are the load and pump efficiency, respectively. The γ_i terms are as follows: 6,768.82 (USD); 202,822.47 (USD/m³); -1,576.96 (USD/m²); 32,576 (USD/m); 994.1 (USD/m²); 3.52 (USD h m⁻¹ kg⁻¹); 0.14 (h²/m⁵); 0.45 (h/m²); 1 dimensionless, 0.54 (m) and 261.61 (USD m h²/kg), respectively.

For the estimation of the costs of the solar collector network, they can also be annualised, a 25-year amortisation period of the investment is considered with fixed interest of 5%, as shown in Eq. (10)

$$C_{TA\ SCN} = f_A C_{SCN} \quad (10)$$

Table 3 shows the arrangement area, and costs of the flat solar collector network where two scenarios are analysed. In scenario 1, it is considered that solar thermal energy supplies the entire thermal load required for the process at a temperature of 101 °C. In scenario two, a limitation of 50% is considered in the area available for the installation of the solar collector network in the plant. The first scenario would be the most desirable where it seeks to substitute the use of fossil fuels in a profitable way. In this scenario, it is also considered that there are no restrictions on available area or capital investment. Scenario 2 has a lower investment, however, there are still emissions to the environment.

2.5 Thermal storage system

The cost of the thermal storage system represents 30% of the cost of the solar thermal installation [17] and its operation is essential to store heat, also to dampen fluctuations in environmental variability, and increase the solar fraction of the process, when there is a gap between energy production and demand.

To determine the size of the thermal storage system, V_{TS} (m^3), we have Eq. (11) [18]:

$$V_{TS} = \frac{3600 Q_{TS} t}{C_p \Delta T_{TS} \rho \text{eff}_{TS}} \quad (11)$$

In Eq. (11), Q_{TS} is the total heat load to be stored in the day (kW), t is the storage time of the system (h), C_p is the heat capacity of the working fluid (kJ/kg °C) and ρ is the density of the thermal fluid (kg/m^3), in this case water, ΔT_{TS} and eff_{TS} are the temperature variation of the thermal storage system (°C) and its efficiency (dimensionless).

The size, storage time and cost of the storage system is conditioned by the sizing of the collector network and the operation of the solar thermal device. Next, Eq. (12) used to determine the cost of storage, C_{TS} (USD) [18].

$$C_{TS} = 5800 + 1600 V_{TS}^{0.7} \quad (12)$$

The cost of the thermal storage system is also annualised with an interest of 5% in a period of 25 years, this function is by Eq. (13) where the cost of the thermal storage system is multiplied by the annualisation factor, f_A .

$$C_{A\ TS} = f_A C_{TS} \quad (13)$$

Heat load to supply (kW)	Temperature level (°C)	Solar collector network array	A_{SCN} (m^2)	f	Supply period (h)	C_{SCN} (USD)	$C_{TA\ SCN}$ (USD/y)
339.81	101.20	23x29	1293.98	1	5	367,412.97	26,068.85
169.91	101.20	12x29	675.12	0.5	5	204,448.15	14,506.10

Table 3.
Results of the design of the solar collector network for different operating conditions.

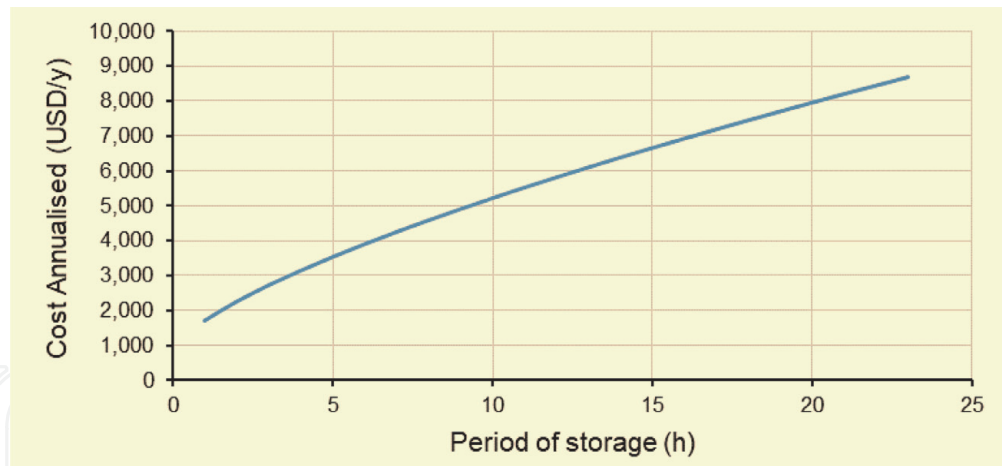


Figure 11.
 Annualised cost of the thermal storage system as a function of accumulation time.

In **Figure 11** the annualised cost of the thermal storage system is shown as a function of the accumulation time, costs increase the longer the storage time. **Figure 11** shows the annualised cost of the thermal storage system for a load of 339,812 kW, which corresponds to the total heating service. If we assume that this thermal load is stored for 23 hours, the cost would be 8669.73 USD/year, compared to the cost of the solar collector network, this represents 32%. To define the operation and size of the storage system, the process conditions and the costs associated with them must be considered.

2.6 Total cost of the solar thermal installation

The total cost of the solar thermal installation (USD) includes: the total cost of the solar collector network and the total cost of the thermal storage system that represents around 80% of the total, the rest corresponds to the control and pumping system. The costs are also annualised at a fixed interest rate (5%) for a repayment period of 25 years and the costs are obtained per year for that period.

2.6.1 Cost evaluation

To evaluate the total cost of the integrated system, the costs of each of the components must first be updated: the heat recovery network, the solar field, and the thermal storage system. In this case the values of the equations are calculated for the year 2010. To obtain the updated cost values, the costs obtained must be multiplied by the value of the ratio that exists between the cost index for 2019 (I_C 2019) and the 2010 cost index (I_C 2010), which are 607.5 and 550.8, respectively [15] as seen in Eq. (14).

$$I_A = \frac{I_C 2019}{I_C 2010} \quad (14)$$

One method of comparing the magnitude of a dollar equity investment with a future stream of income is to convert the cost of capital into a future annual charge. The calculation is done with Eq. (15) [15], where i is the annual interest and n is the number of years of useful life of a piece of equipment or of a network of equipment or process in general. According to IRENA, solar plants have a useful life of 25 years.

$$f_A = C_T * \left[\frac{i * (1 + i)^n}{(1 + i)^n - 1} \right] \quad (15)$$

2.6.2 Environmental impact assessment

Currently, solar thermal technology is competitive against those that operate with fossil fuels, however, the negative environmental impact generated by these energy sources is global and tangible. One of the most well-known parameters is the quantification of CO₂ emissions as greenhouse gas, however, they are not the only gases emitted, in addition, there are other no less important parameters that are not considered. In this study, only the tons of CO₂ that are ceased to be emitted into the atmosphere are quantified when integrating solar thermal energy into the process. The factor of 0.203 kg CO₂/kWh is considered for fixed combustion equipment that works with natural gas as fuel, this data is reported for the European Union [19].

3. Analysis of results

The original energy consumption of the process is 880.202 kW for 5 h/day with a generation of CO₂ emissions of 312.7 tons/year (893.40 kg/day). The average price of natural gas reported worldwide for 2020 was 0.047 USD/kWh [20]. While the reported price of the same fuel in Mexico, for first month of 2019, was 0.3589 USD/kWh [21]. As can be seen, they present a significant difference that will directly impact the investment recovery time. It should be noted that the price of natural gas in Mexico has varied significantly from January 2019 (0.3589 USD/kWh) to December 2020 (0.024 USD/kWh).

When analysing the match between the energy requirement of the process and the availability of solar energy, it was determined that it is 2 h. However, there is availability of solar thermal energy at the target temperature for 1 h more that can be used as most convenient in the operation of the solar thermal device. To supply the entire thermal load and cover the remaining three hours, a storage tank of 32.58 m³ is required.

In scenario 1 it is considered that there are no restrictions due to limitation of available area and capital investment. When carrying out the integration of energy, the requirement of the hot utility is reduced by 61.4%, the rest can be provided with solar thermal energy and the generation of greenhouse gases is zero. The total cost of the integrated system (heat recovery network and solar thermal installation) is 1,995,266.49 USD. If the investment is made for 25 years, the cost is 145,488.85 USD/year. The payback for the integrated system is 27.56 years (according to international data) and 3.6 years (Mexican data). When considering only the solar thermal installation, the payback is 5.99 years (according to the international estimate) and 0.78 years (according to the national evaluation).

In scenario 2 there is an available area restriction of 50% (650 m²). The resulting network, depending on the available space, presents an arrangement of 11x29 with a thermal load of 181.45 kW that can supply 2 h of the thermal requirement of the process. The supply of the thermal load for those 2 h can be given directly from 11:00 h - 13:00 without storage or, it can be supplied from 8:00 h - 10:00 h with storage. Based on the economic aspect for scenario 2, the supply of the thermal load will be for 2 h without storage. The cost of the integrated system is 1,750,541.36 USD with a reduction of 12% compared to scenario 1. CO₂ emissions into the atmosphere are 60.36 tons/year. The payback of the integrated system is 24.17 years (according to the international price of gas) and 3.166 years (according to the national price of gas). The payback of the solar collector network is 2.61 years (according to the international gas price report) and 0.34 years (for the national gas price reported).

4. Chemical vapour deposition as a route to improve solar technology

Other solar technology that is heading the solar integration to industry in a big part of world, are the photovoltaic solar panels. Photovoltaics (PV) implies the direct conversion of sunlight into electricity by mean of semiconducting materials with a photovoltaic effect. Solar panels are widely used because its property of magnify the inlet micro-power, by the relatively constant production of electricity and by the possibility to use the stored electrical energy even in the absence of sunlight. Each solar panel is made up of a multitude of solar cells which manufacturing is, in this moment, in a high-tech period (third generation) of research (i. e. Dye-sensitised solar cells, DSSC, Perovskite solar cells, PVSC, Polymer hetero-junction solar cells, PSC, among others) [4]. Function, materials, characteristics, power-conversion-efficiency of solar cells are widely described in meticulous reviews and papers [4, 22–23]. The aim in this paragraph is to display the benefits that use of Chemical Vapour Deposition, CVD, has implied to improve solar cells performance and to present the novelties in evacuated solar tubes.

Among the most used thin film deposition processes to manufacture solar cells, are: evaporation, sputtering technique and chemical vapour deposition (CVD), with some variants in each technique. Briefly, they can be described as follows [24]:

Evaporation. The source material is evaporated in vacuum, this lets vapour particles to travel until the substrate, then, they condense to a solid state. Unfortunately, could occur that the different components of an alloy vaporise at different speeds, which will cause the composition of the deposited layer to be different from the original composition.

Sputtering deposition or Physical Vapour Deposition. The source materials are sputtered by the hitting of high energy ions in an oxidising atmosphere and deposited on a heated substrate, following the growth of thin films.

Chemical Vapour Deposition (CVD). The CVD technique consists of the reaction of a gas mixture inside a vacuum chamber followed by diffusion of reactants to a heated substrate to produce a material in the form of a thin layer. A useful variant is the reaction of metal–organic precursors (MO-CVD) because these ones improve the efficiency of solar cells.

Using CVD and PVD techniques give added value to solar cells with not too high costs, thanks to these techniques the efficiency of solar cells has increased from 10% in the 70ies to 20% today, since the different thin films that can be deposited perform various functions such as: antireflection, passivation layers, thickening of the absorbent layer, among others that have not yet been explored [24].

It is important to mention that exists an innovative report in literature about the use of CVD technique to deposite selective coating in evacuated solar tubes. The novel absorber layers have a base of carbon nanotube sheets that have showed their capability to converting solar radiation into electricity and heat [25], this is a promising result in increasing the efficiency of evacuated tubes.

5. Conclusions

The proposed methodology allows integrating solar thermal energy, in a profitable way, and replace, totally, the use of fossil fuels (scenario 1).

In the event of any restriction such as an available space of 50% respect scenario 1 (scenario 2), cost savings can be up to 12% during the two hours that the thermal load can be supplied directly, with a payback time of the solar device of 2.61 years, eliminating completely the use of thermal storage. The reduction of the requirement of hot utility was 80.62% being 19.40% by integration from solar energy.

Whenever solar energy is integrated, there is a reduction in greenhouse gas emissions, but when the first objective is to reduce GHG, there should be no limitation in the economic aspect to achieve the objective. Because current international prices of conventional fuels constitute a determining restriction to integrate solar heat to industrial processes. Therefore, economic speculation of conventional fuel prices constitutes a relevant challenge to be considered in the proposal and implementation of energy policies that really intend to encourage business models with renewables, and more specifically, with solar thermal energy.

Acknowledgements

The authors are very grateful to the University of Guanajuato and Trade Union Association, ASPAAUG, for the partial support granted for the publication costs of this chapter.

Conflict of interest

The authors declare no conflict of interest.

Nomenclature

A_{HRN}	Area of the heat recovery network, m^2 .
A_{SCN}	Area of the solar collector network, m^2 .
A_t	Lateral area of the tube, m^2 .
C_{HRN}	Cost of the heat recovery network, USD.
C_{AS}	Cost of auxiliary services, USD/year.
C_{ATS}	Annualised cost of the thermal storage system, USD/year.
C_{CO}	Costs associated with cooling water, USD/kW year.
C_{SCN}	Cost of the collector network, USD.
C_{ST}	Costs associated with steam, USD/kW year.
$C_{TA HRN}$	Cost of the annualised heat recovery network, USD/year.
$C_{TA SCN}$	Annualised costs of the solar collector network, USD/year.
C_{TS}	Cost of the system storage thermal, USD.
C_p	Heat capacity of the working fluid, $kJ/kg^\circ C$.
CP	Mass flow multiplied by the specific heat of the stream, $kW/^\circ C$.
d	Internal diameter of a tube of the solar collector, m.
eff	Pump efficiency, dimensionless.
eff_{TS}	Efficiency, dimensionless.
f_A	Annualisation factor, dimensionless.
h_i	Heat transfer coefficient of i-th stream, $kW/m^2^\circ C$.
h_j	Heat transfer coefficient of j-th stream, in $kW/m^2^\circ C$.
H_b	Load pump, m.
i	Annual interest, %.
$I_{C 2010}$	Cost index for 2010, dimensionless.
$I_{C 2019}$	Cost index for 2019, dimensionless.
L	Length of the solar collector, m.
\dot{m}	Mass flow rate, kg/s .
n	Number of years, y.
N_c	Number of solar collectors, dimensionless.
N_e	Number of equipment, dimensionless.

N_p	Number of branches or lines in parallel, dimensionless.
N_s	Number of series collectors, dimensionless.
N_t	Number of tubes, dimensionless.
q_i	Enthalpy change of i-th stream, kW.
q_j	Enthalpy change of j-th stream, kW.
Q	Total thermal load required by the process, kW.
Q_c	Minimum requirements for cooling the process, kW.
Q_h	Minimum requirements for heating, kW.
Q_i	Thermal load provided by a series of n collectors connected in series, kW.
Q_{TS}	Total heat load to be stored, kW.
t	Storage time of the system, h.
T_i	Temperature of the fluid at the entrance to the collector, °C.
T_{inlet}	Stream inlet temperature, °C.
T_o	Outlet temperature of the fluid from the collector, °C.
T_o^n	Outlet temperature of the n-th element, °C.
T_o^{n-1}	Outlet temperature of one minus to the n-th element, °C.
T_{outlet}	Stream outlet temperature, °C.
V_{TS}	Volume of the thermal storage system, m ³ .
W	Width of the solar collector, m.
Greek symbols	
ΔT	Temperature difference, °C.
ΔT_{min}	Delta temperature minimum, °C.
ΔT_{ML}	Logarithmic mean temperature difference, °C.
ΔT_{TS}	Delta temperature variation of the thermal storage system, °C.
γ_0	Materials adjustment parameter, 6768.82 USD.
γ_1	Raisers adjustment parameter, 202,822.47 USD/m ³ .
γ_2	Raisers diameter adjustment parameter, 1576.96 USD/m ² .
γ_3	Raisers diameter adjustment parameter, 32.576 USD/m.
γ_4	FPSC area adjustment parameter, 994.1 USD/m ² .
γ_5	Pumping costs adjustment parameter, 3.52 USD h/m kg.
γ_6	Pumping costs adjustment parameter, 0.14 h ² /m ⁵ .
γ_7	Pumping costs adjustment parameter, 0.45 h/m ² .
γ_8	Pumping costs adjustment parameter, 1.00 dimensionless.
γ_9	Pumping costs adjustment parameter, 0.54 m.
γ_{10}	Pumping costs adjustment parameter, 261.61 USD m h ² /kg.
ρ	Density of the thermal fluid, kg/m ³ .

IntechOpen

IntechOpen

Author details

Guillermo Martínez-Rodríguez* and Amanda L. Fuentes-Silva
Department of Chemical Engineering, University of Guanajuato, Guanajuato,
Mexico

*Address all correspondence to: guimarod@ugto.mx

IntechOpen

© 2021 The Author(s). Licensee IntechOpen. This chapter is distributed under the terms of the Creative Commons Attribution License (<http://creativecommons.org/licenses/by/3.0>), which permits unrestricted use, distribution, and reproduction in any medium, provided the original work is properly cited. 

References

- [1] World Energy Outlook 2016, OECD/IEA [Internet]. 2016. Available from: <https://www.iea.org/reports/world-energy-outlook-2016> [Accessed: 2020-12-01]
- [2] Schoeneberger C, McMillan CA, Kurup P, Akar S, Margolis R, Masanet E. Solar for industrial process heat: A review of technologies, analysis approaches, and potential applications in the United States. *Energy*. 2020; 206:118083. DOI: 10.1016/j.energy.2020.118083
- [3] International Renewable Energy Agency (IRENA), calculations made by Deger Saygin based on the source International Energy Agency (IEA), World Energy Statistics 2018 [Internet]. 2018. Available from: https://www.irena.org/-/media/Files/IRENA/Agency/Publication/2018/Jul/IRENA_Renewable_Energy_Statistics_2018.pdf [Accessed: 2020-12-01]
- [4] Babar F, Mehmood U, Asghar H, Mehdi M H, Khan A U H, Khalid H, Huda N U, Fatima Z. Nanostructured photoanode materials and their deposition methods for efficient and economical third generation dye-sensitized solar cells: A comprehensive review. *Renewable and Sustainable Energy Reviews*. 2020; 129: 109919. DOI: 10.1016/j.rser.2020.109919
- [5] Baniassadi A, Momen M, Amidpour M, Pournali O. Modeling, and design of solar heat integration in process industries with heat storage. *Journal of Cleaner Production*. 2018; 170: 522–534. DOI: 10.1016/j.jclepro.2017.09.183
- [6] Oosthuizen D, Jurgens Goosen N, Hess S. Solar thermal process heat in fishmeal production: prospects for two South African fishmeal factories. *Journal of Cleaner Production*. 2020; 253: 119818. DOI: 10.1016/j.jclepro.2019.119818
- [7] Jia T, Huan J, Li R, He P, Dai Y. Status, and prospect of solar heat for industrial processes in China. *Renewable and Sustainable Energy Reviews*. 2018; 90: 475–489. DOI: / 10.1016/j.rser.2018.03.077
- [8] Fuentes-Silva AL, Velázquez-Torres D, Picón-Núñez M, Martínez-Rodríguez G. Solar Thermal Integration With and Without Energy Storage: The Cases of Bioethanol and a Dairy Plant. *Chemical Engineering Transactions*. 2020; 81: 493–498. DOI:10.3303/CET2081083.
- [9] Denholm P, Brinkman G, Mai T. How low can you go? The importance of quantifying minimum levels for renewable integration generation. *Energy Policy*. 2018; 115: 249–257. DOI: 10.1016/j.enpol.2018.01.023
- [10] Eiholzer T, Olsen D, Hoffman D. Integration of a solar thermal system in a medium-sized brewery using pinch analysis: methodology and case study. *Applied Thermal Engineering*. 2017; 113: 1558–1568. <http://dx.doi.org/10.1016/j.applthermaleng.2016.09.124>.
- [11] Suresh N, Rao BS. Solar energy for process heating: a case study of select Indian industries. *Journal of Cleaner Production*. 2017. 151: 439–451. DOI: 10.1016/j.jclepro.2017.02.190
- [12] Quijera JA, González-Alriols M, Labidi J. Integration of a solar thermal system in a dairy process. *Renewable Energy*. 2011; 36: 1843–1853. DOI: 10.1016/j.renene.2010.11.029.
- [13] Linnhoff, B. Linnhoff March: Introduction to Pinch Technology [Internet]. 1998. Available from: <https://www.ou.edu/class/che-design/a-design/Introduction%20to%20Pinch%20Technology-LinhoffMarch.pdf> [Accessed: 2020-12-05]

- [14] Smith R. Chemical Process Design and Integration. In John Wiley & Sons, Ltd. 2005.
- [15] Towler G, Sinnott R. Chemical Engineering Design. 2nd ed. Oxford: Butterworth-Heinemann/Elsevier; 2013. 1320 p. DOI: 10.1016/C2009-0-61216-2
- [16] Martínez-Rodríguez G, Fuentes-Silva AL, Lizárraga-Morazán JR, Picón-Núñez M. Incorporating the concept of flexible operation in the design of solar collector fields for industrial applications. *Energies*. 2019; 12: 570: 1–20. DOI: 10.3390/en12030570.
- [17] Karagiorgias M, Botzios A, Tsoutsos T. Industrial solar thermal applications in Greece economic evaluation, quality requirements and case studies. *Renewable and Sustainable Energy Reviews* 2001; 5: 157–173. DOI: 10.1016/S1364-0321(00)00012-5.
- [18] Yang P, Liu LL, Du J, Li JL, Meng QW. Heat exchanger network synthesis for batch processes by involving heat storages with cost targets. *Applied Thermal Engineering*. 2014; 70, 1276–1128. DOI: 10.1016/j.applthermaleng.2014.05.041
- [19] Emission factors carbon footprint registration, offsetting, and carbon dioxide absorption projects version 12nd, Spanish Office for Climate Change (OECC) [Internet]. 2019. Available from: https://www.miteco.gob.es/es/cambio-climatico/temas/mitigacion-politicas-y-medidas/factores_emision_tcm30-479095.pdf [Accessed: 2020-12-01]
- [20] Global Petrol Prices [Internet]. 2020. Available from: https://es.globalpetrolprices.com/Mexico/natural_gas_prices/ [Accessed: 2021-02-12]
- [21] Comisión Reguladora de Energía (CRE) [Internet]. 2021. Available from: <https://www.cre.gob.mx/IPGN/index.html> [Accessed: 2021-02-12]
- [22] Tao F, Green M, Valenzuela-Garcia A, Xiao T, Van-Tran A T, Zhang Y*, Yin Y, Chen X. Recent progress of nanostructured interfacial solar vapor generators. *Applied Materials Today*. 2019; 17: 45–84. DOI: 10.1016/j.apmt.2019.07.0112352-9407
- [23] Dapkus P D*, Chi C Y, Choi S J, Chu H J, Dreiske M, Li R, Lin Y, Nakajima Y, Ren D, Stevenson R, Yao M, Yeh T W, Zhao H. Selective area epitaxy by metalorganic chemical vapor deposition—a tool for photonic and novel nanostructure integration. *Progress in Quantum Electronics*. DOI: 10.1016/j.pquantelec.2020.100304
- [24] Hoffmann W, Pellkofer T. Thin films in photovoltaics: Technologies and perspectives. *Thin Solid Films*. 2012; 520: 4094–4100. DOI: 10.1016/j.tsf.2011.04.146
- [25] Sobhansarbandi S, Martinez P M, Papadimitratos A, Zakhidov A, Hassanipour F. Evacuated tube solar collector with multifunctional absorber layers. *Solar Energy*. 2017;146: 342–350. DOI: 10.1016/j.solener.2017.02.038